DALTON
FULL PAPER

Structures and spectra of bis-tripodal iron(II) chelates, $[FeL_2]^{2+}$, where L = tris(pyrazol-1-yl)methane, tris(pyridin-2-yl)methane, bis(pyrazol-1-yl)(pyridin-2-yl)methane and tris(pyridin-2-yl)-phosphine oxide. Magnetism and spin crossover in the $(pz)_3CH$ case

Peter A. Anderson,[a] Timothy Astley,[b] Michael A. Hitchman,[b] F. Richard Keene,[a] Boujemaa Moubaraki,[c] Keith S. Murray,*[c] Brian W. Skelton,[d] Edward R. T. Tiekink,[e] Hans Toftlund[f] and Allan H. White[d]

[a] *School of Biomedical & Molecular Sciences, James Cook University, Townsville, Queensland 4811, Australia*
[b] *School of Chemistry, University of Tasmania, GPO Box 252-75, Hobart, Tasmania 7001, Australia*
[c] *Department of Chemistry, PO Box 23, Monash University, Victoria 3800, Australia. Fax: +61 3 9905 4597; E-mail: Keith.S.Murray@sci.monash.edu.au*
[d] *Chemistry Department, University of Western Australia, Nedlands, WA 6907, Australia*
[e] *Department of Chemistry, University of Adelaide, Adelaide, SA 5005, Australia*
[f] *Chemistry Department, University of Southern Denmark, Odense M, DK 5230, Denmark*

Received 25th April 2000, Accepted 15th August 2000
First published as an Advance Article on the web 19th September 2000

A range of six-co-ordinate bis-tripodal iron(II) chelates, $[FeL_2]^{2+}$, has been synthesized from iron-(II) or -(III) precursors where L = tris(pyrazol-1-yl)methane $(pz)_3CH$, tris(pyridyl-2-yl)methane $(py)_3CH$, bis(pyrazol-1-yl)-(pyridin-2-yl)methane $(pz)_2(py)CH$ and tris(pyridin-2-yl)phosphine oxide $(py)_3P{=}O$. Crystal structures have been determined for three compounds and in the $(pz)_3CH$ case for two polymorphs (α and β) which were obtained in two different laboratories from iron(III) salts using different crystallisation solvents. The electronic properties of the $[FeL_2]^{2+}$ series have been investigated by optical spectroscopic measurements. Low-spin d^6 behaviour is indicated. Magnetic and Mössbauer effect measurements on $[Fe\{(pz)_3CH\}_2]^{2+}$ show that a gradual spin crossover to the high-spin state occurs above 270 K, though this is far from developed at 350 K. Comparisons are made with the well studied boron ligand analogue $[Fe\{(pz)_3BH\}_2]$, which displays similar crossover behaviour, and with bis(tridentate) ligand complexes containing the ligand 1,4,7-triazacyclononane.

In comparison to the large number of studies reported for hydridotris(pyrazol-1-yl)borate complexes of iron(II),[1] comparatively little is known on the neutral ligand analogues such as tris(pyrazol-1-yl)methane and its congeners. McGarvey, Toftlund and co-workers[2] reported preliminary susceptibility *versus* temperature data for the low-spin $[Fe\{(pz)_3CH\}_2]Y_2$ where $Y = ClO_4^-$ and a study of the photoperturbation of the $^1A_1 \longleftrightarrow {}^5T_2$ equilibrium in acetonitrile solution, *via* ligand-field excitation. Mössbauer spectroscopy also provided evidence for spin-state isomerism occurring in the solid state for $Y = PF_6$.[3] Hitchman and co-workers reported[4] a visible-spectral and angular overlap study of metal to ligand bonding in the related unsymmetrical tripodal system $[M\{(pz)_2(py)CH\}_2][NO_3]_2$, where M = Fe, Ni, Co or Cu, and found that the ligand produced a large ligand field splitting, with the pyridine being a stronger σ donor than the pyrazole, and both the pyridine and pyrazole groups acting as weak π donors. The π-acceptor properties of a series of related tripodal ligands containing 2-pyridyl substituents (*viz.* $(py)_3CH$, $(py)_3COH$, $(py)_3N$, $(py)_3P$, and $(py)_3P{=}O$) attached to Co^I and Ru^{II} have been reported by Keene *et al.*[5]

In the present paper we report the crystal structures of α and β polymorphs of $[Fe\{(pz)_3CH\}_2][NO_3]_2$ and of $[Fe\{(py)_3CH\}_2][NO_3]_2$ and $[Fe\{(py)_3PO\}_2][NO_3]_2$. A detailed discussion of the visible spectra, bonding and electrochemistry of these compounds is provided. Variable temperature magnetic measurements are restricted to the $(pz)_3CH$ compound. Comparisons are made, where appropriate, with the properties of the related bis(tridentate) $[Fe\{(pz)_3BH\}_2]$ and $[Fe([9]aneN_2S)_2]^{2+}$[6] compounds where $[9]aneN_2S$ is 1-thia-4,7-diazacyclononane. Some preliminary aspects of the present work have been presented elsewhere.[2,7]

Experimental

Except where indicated, syntheses of iron(II) complexes were carried out in air using laboratory grade solvents and iron salts. Tris(pyrazol-1-yl)methane $(pz)_3CH$,[8] tris(pyridin-2-yl)methane $(py)_3CH$,[5] and bis(pyrazol-1-yl)(pyridin-2-yl)methane $(pz)_2(py)CH$[9] were prepared by reported methods.

Syntheses

$[Fe^{II}\{(pz)_3CH\}_2][ClO_4]_2$. $Fe^{III}(ClO_4)_3{\cdot}6H_2O$ (0.64 g, 1.4 mmol) was added to a stirred solution containing tris(pyrazol-1-yl)-methane (0.43 g, 2 mmol) dissolved in methanol–acetone (1 : 1). Clear pink crystals of the iron(II) complex were deposited. Found: C, 35.4; H, 3.0; Cl 10.1; N, 24.3. $C_{20}H_{20}FeCl_2N_{12}O_8$ requires: C, 35.2; H, 2.9; Cl, 10.4; N, 24.6%). μ_{Fe} (295 K) = 1.51 μ_B. Mössbauer spectrum (4.2 K relative to α-Fe): $\delta = 0.488$ mm s^{-1}, $\Delta E_Q = 0.248$ mm s^{-1}. The same pink product could be

obtained on slow recrystallisation of the brown $[Fe^{III}\{(pz)_3CH\}_2][ClO_4]_3$ complex (described below) by diffusing hexane into an acetonitrile solution. A green side product $[\{(pz)_3CH\}Fe^{III}(\mu\text{-}O)(\mu\text{-}HCO_2)_2Fe^{III}\{(pz)_3CH\}][ClO_4]_2$ (to be described elsewhere[10]) was also obtained in this recrystallisation process. $[Fe^{II}\{(pz)_3CH\}_2][ClO_4]_2$ has also been synthesized by reaction of $Fe(ClO_4)_2\cdot 6H_2O$ with ligand in ethanol under anaerobic conditions.

$[Fe^{II}\{(pz)_3CH\}_2][NO_3]_2$ (α form) 1. This complex was made in a similar way to the ClO_4^- salt, starting from $Fe^{III}(NO_3)_3\cdot 9H_2O$. It is more soluble than the ClO_4^- salt. Crystals of **1** suitable for X-ray diffraction studies were obtained by slow evaporation of an aqueous solution of the iron(II) complex. Repeat syntheses yielded bulk samples having identical powder X-ray diffraction patterns to those observed for bulk samples of **2** below, and those calculated from the crystal co-ordinates of **2**. The α form is therefore obtained as a minor product.

$[Fe^{II}\{(pz)_3CH\}_2][NO_3]_2$ (β form) 2. A solution of $Fe(NO_3)_3\cdot 9H_2O$ in acetone was added to a solution of $(pz)_3CH$ in the same solvent with a molar ratio of 1:2. A red precipitate formed which, after filtration, was recrystallised by diethyl ether vapour diffusion into an acetonitrile solution to yield well formed red crystals of **2**. Found: C, 39.8; H, 3.2; N, 32.0. $C_{20}H_{20}FeN_{14}O_6$ requires: C, 39.5; H, 3.3; N, 32.2%).

$[Fe^{II}\{(py)_3CH\}_2][PF_6]_2$. Under an argon atmosphere, $FeSO_4\cdot 5H_2O$ (37.5 mg, 0.15 mmol) was dissolved in water (5 ml), and the solution added to an ethanolic (5 ml) solution of tris(pyridin-2-yl)methane (0.102 g, 0.4 mmol). An orange solution was formed and the cation precipitated by addition of solid NH_4PF_6. The solid was collected by filtration, washed three times with cold water and dried *in vacuo*. Yield 0.11 g, 85%.

$[Fe^{II}\{(py)_3CH\}_2][NO_3]_2$ 3. A portion of the complex $[Fe^{II}\{(py)_3CH\}_2][PF_6]_2$ was dissolved in a minimum volume of water and solid $LiNO_3$ added. The resultant red-orange precipitate was collected by centrifugation and recrystallised by liquid diffusion of ether into an acetonitrile solution. Found: C, 56.8; H, 4.10; N, 16.8. $C_{32}H_{26}FeN_8O_6$ requires: C, 57.0; H, 3.89; N, 16.6%.

$[Fe^{II}\{(pz)_2(py)CH\}_2][PF_6]_2$. This complex was prepared (73% yield) in an analogous manner to $[Fe^{II}\{(py)_3CH\}_2][PF_6]_2$ (see above), using an acetone solution of the ligand.

$[Fe^{II}\{(pz)_2(py)CH\}_2][NO_3]_2$. This was obtained by a method reported previously, starting from $Fe^{III}(NO_3)_3\cdot 9H_2O$,[4] and crystals satisfactory for X-ray diffraction studies were obtained by vapour diffusion of diethyl ether into an acetonitrile–methanol (1:1) solution of the complex.

$[Fe^{II}\{(py)_3P{=}O\}_2][NO_3]_2$ 4. Under an argon atmosphere, a methanolic solution of $Fe(NO_3)_3\cdot 9H_2O$ was added to a solution of a two molar amount of tris(pyridin-2-yl)phosphine in methanol. The resulting orange precipitate was recrystallised by liquid diffusion of diethyl ether into an acetonitrile solution. A diacetonitrile solvate was obtained (see X-ray section) in 70% yield. Found: C, 49.2; H, 3.60; N, 17.2. $C_{30}H_{30}FeN_{10}O_8P_2$ requires: C, 49.5; H, 3.67; N, 17.0%.

$[Fe^{III}\{(pz)_3CH\}_2][ClO_4]_3$. This iron(III) complex was prepared using the same method as for the iron(II) analogue, but with methanol as solvent. The dark brown product precipitated immediately on mixing the reagents. It was stirred for 10 min, filtered off, washed successively with ethanol (50 ml) and diethyl ether (50 ml) and dried in vacuum. Yield 0.6 g, 76%. Found: C, 30.2; H, 2.4; N, 20.4. $C_{20}H_{20}Cl_3FeN_{12}O_{12}$ requires: C, 30.7; H, 2.5; N, 21.5%. It could be crystallised as dark maroon crystals by diffusing diethyl ether into a saturated solution of the complex dissolved in CH_3CN. Such crystals lost solvent molecules rapidly. μ_{Fe} (295 K) = 2.7 μ_B. Mössbauer spectrum (295 K, relative to α-Fe): $\delta = 0.05$ mm s^{-1}, $\Delta E_Q = 0.82$ mm s^{-1}. Visible spectrum, (CH_3CN): 21459 and 17860 (sh) cm^{-1}.

Electrochemistry

Cyclic voltammetric studies were undertaken with a BAS 100 Electrochemical Analyzer. Studies at Monash University on the $(pz)_3CH$ complexes were undertaken at room temperature in acetonitrile solution at a platinum working electrode with a saturated calomel electrode as reference and 0.1 M n-Bu_4NClO_4 as supporting electrolyte. The scan rate was 300 mV s^{-1}. Under these conditions the ferrocene–ferrocenium couple was +0.42 V relative to SCE. Studies at James Cook University on $[Fe\{(py)_3CH\}_2][PF_6]_2$ and $[Fe\{(pz)_2(py)CH\}_2][PF_6]_2$ were performed in acetonitrile–0.1 M n-Bu_4NPF_6 solution under argon, at a platinum working electrode with a Ag–$AgNO_3$ (0.01 M) reference electrode and a scan rate of 100 mV s^{-1}. The potential of the SCE electrode is −0.31 V relative to Ag–Ag^+.

Magnetic studies

Magnetic susceptibility studies were made using a Quantum Design MPMS Squid magnetometer with an applied field of 1 T. The powdered sample was contained in a calibrated gelatine capsule held in the centre of a drinking straw fixed to the end of the sample rod. The magnetisation values of the instrument were calibrated against a standard palladium sample supplied by Quantum Design, and also by use of chemical calibrants such as $CuSO_4\cdot 5H_2O$ and $[Ni(en)_3][S_2O_3]$ (en = ethane-1,2-diamine).

Electronic spectroscopy

Single-crystal and KBr disk electronic spectra were recorded using either a Cary 17 or 5 spectrophotometer by a procedure described in detail elsewhere,[11] with the samples cooled using a Cryodyne model 22C cryostat. Absorption coefficients were estimated by measuring crystal thickness using a microscope with a graduated eyepiece. Solution spectra were measured on a Cary 5G spectrophotometer using CH_3CN or DMF as solvent for complex **1** and with a Cary 17 spectrophotometer using methanol as solvent for **3** and **4**.

Mössbauer spectroscopy

Mössbauer spectra were measured by Associate Professor J. D. Cashion, Physics Department, Monash University, with a standard electromechanical transducer operating in a symmetrical constant-acceleration mode. A conventional helium bath cryostat was employed for temperature control with the sample maintained in exchange gas. Spectra were collected with an LSI-based 1000-channel multianalyser. Velocity calibration was made with respect to α-iron foil. Spectra were fitted using Lorentzian lineshapes.

Structure determinations

Crystal data measurements and refinements were carried out for both forms of $[Fe^{II}\{(pz)_3CH\}_2][NO_3]_2$ **1** (α-form) and **2** (β-form) at the University of Western Australia and for $[Fe\{(py)_3CH\}_2][NO_3]_2$ **3** and $[Fe\{(py)_3PO\}_2][NO_3]_2\cdot 2CH_3CN$ **4** at the University of Adelaide.

Unique room-temperature four-circle/single counter diffractometer data sets were measured (ω–2θ scan mode, $2\theta_{max}$ as specified, monochromated Mo-Kα radiation, $\lambda = 0.7107_3$ Å; T *ca.* 295 K) yielding N independent reflections, N_o with $I > 3\sigma(I)$ being considered 'observed' and used in the full-matrix least squares refinement after absorption correction. Anisotropic thermal parameters were refined for the non-hydrogen atoms, (x, y, z, U_{iso})$_H$ being refined for complexes **1**,**2** and constrained

at estimated values for **3**, **4**. Conventional residuals, R, R_w (statistical weights) are quoted at convergence, neutral atom complex scattering factors being employed. Pertinent results and data are given in Tables 1 and 2 and Figs. 1 and 2, the latter showing thermal ellipsoid amplitudes at the 20% (50% for **3**, **4**) probability level and hydrogen atoms with arbitrary radii of 0.1 Å. Individual difficulties, idiosyncrasies, abnormalities, variations in procedure (*etc.*) are cited as footnotes in Table 1. Computation used the XTAL 3.0 program system for **1**, **2** [12] and TEXSAN [13] for **3**, **4**.

CCDC reference number 186/2146.

See http://www.rsc.org/suppdata/dt/b0/b003299i/ for crystallographic files in .cif format.

Powder X-ray diffraction studies

A Scintag diffractometer was employed to obtain diffractograms on bulk samples of complexes **1** and **2**. The wavelength used was 1.54059 Å.

Results and discussion

Synthesis

While the iron(II) complexes can be synthesized from iron(II) salts under an inert atmosphere, one of the interesting features of these compounds was that they were also obtained, even in air, starting from an iron(III) precursor. We have not explored this redox reaction in any detail but it appears to be solvent dependent. Thus, for L = $(pz)_3CH$, reaction of a hydrated iron(III) salt in methanol led to rapid isolation of the $[Fe^{III}\{(pz)_3CH\}_2]^{3+}$ complex as a brown-maroon crystalline solid which, unfortunately, has not yet proved accessible to X-ray study. Kinetic effects are therefore important in methanol. The cyclic voltammogram of the iron(III) complex (see below) is identical upon reductive sweep to that of $[Fe^{II}\{(pz)_3CH\}_2]^{2+}$ obtained on oxidative sweep. Slow recrystallisation of $[Fe^{III}\{(pz)_3CH\}_2][ClO_4]_3$ in CH_3CN, in air, led to formation of a mixture of pink crystals of the iron(II) complex and green crystals of a dinuclear μ-oxo, μ-formato iron(III) complex, $[\{(pz)_3CH\}Fe^{III}(\mu\text{-}O)(\mu\text{-}HCO_2)_2Fe^{III}\{(pz)_3CH\}][ClO_4]_2$,[10] the formate presumably originating from hydrolysis of $(pz)_3CH$ rather than from oxidation of methanol (by Fe^{III}). When acetone or acetone–methanol were used as solvent only the $[Fe^{II}\{(pz)_3CH\}_2]^{2+}$ complex was isolated, a situation mirrored with the $(pz)_2py$ ligand. However, use of methanol and L = $(py)_3P$ with Fe^{III} led to reduction to Fe^{II} and conversion of $(py)_3P$ to form $(py)_3P{=}O$, the latter oxidation being common in triarylphosphines and often involving peroxide or O_2 as oxygen transfer reagent. Interestingly, in this case $[Fe^{II}\{(py_3P{=}O\}_2]^{2+}$ was the only isolable species even when the reaction was performed under anaerobic conditions. No $(py)_3P{=}O$ was detectable in the $(py)_3P$ ligand sample used in this synthesis, and the mechanism of ligand oxidation during the synthesis is not understood.

The sign and size of the $E_{1/2}$ values obtained for these $[FeL_2]^{3+/2+}$ couples (*ca.* +1.1 V *vs.* SCE in CH_3CN) are such that they are delicately poised to stabilise the iron(II) form, much as in $[Fe(bipy)_3]^{3+/2+}$ (*ca.* +0.86 V *vs.* SCE in water), with π-acceptor properties of L and ligand-field stabilisation energies playing a part. Other recent examples of iron(II) chelates being formed from iron(III) precursors include those containing ligands such as chloroanilate [14] and oxalates,[15] the latter by photochemical means.

Electrochemistry

The $E_{1/2}$ values for the Fe^{III}–Fe^{II} couple are 0.71 and 0.73 V (*vs.* $Ag–Ag^+$) for $[Fe\{(py)_3CH\}_2]^{n+}$ and $[Fe\{(pz)_2(py)CH\}_2]^{n+}$ respectively (*i.e.* 1.02 and 1.04 V *vs.* SCE) at a platinum working electrode in acetonitrile–0.1 M n-Bu_4NPF_6 solution (see Experimental section for conditions used). In both cases the peak separation ΔE_p was 70 mV and $i_{pa}/i_{pc} \approx 1$, so they are essentially reversible electron transfer processes. $[Fe\{(pz)_3CH\}_2]^{n+}$ behaves similarly with $E_{1/2} = 1.09$ V *vs.* SCE and $\Delta E_p = 80$ mV. In comparison, the classical redox reagent $[Fe(bipy)_3]^{3+/2+}$ has $E_{1/2} = 1.06$ V *vs.* SCE.[16]

Coulometry was carried out under argon to attempt to ascertain why the iron(II) complexes were usually obtained regardless of the initial oxidation state of the iron in the syntheses. A solution of $[Fe\{(pz)_2(py)CH\}_2]^{n+}$ in acetonitrile–0.1 M n-Bu_4NPF_6 solution was taken through a series of bulk electrolyses in turn at 0.85 (oxidation) and 0.65 V (reduction): it was observed that the charge passed in the successive electrolyses remained virtually constant, which would indicate that the iron-(II) and -(III) oxidation states are both stable, at least on the timescale of the coulometry experiment (*ca.* 30 min). The preference for Fe^{II} observed in the syntheses of this series of complexes therefore is related to the solvent used, kinetic effects and the bonding properties of these pyrazole- and pyridyl-based ligands.

Structure determinations

All four complexes structurally characterised are similar and of the form $[Fe\{(ar)_3X\}_2][NO_3]_2\cdot(solv)$, crystallising in the monoclinic space group C_{2h}^5, set as $P2_1/n$ throughout, all with $Z = 2$, so that one half of the centrosymmetric cation, disposed with its iron atom on a crystallographic inversion centre, is crystallographically independent, together with one anion (and one solvent molecule, in one case) making up the asymmetric unit of the structure. All cations have putative $\bar{3}m$ symmetry, the three aromatic planes of each ligand being essentially parallel to the X···Fe···X axis of the cation. Cation geometries for the three independent types are summarised in Table 2, 'equivalent' distances and angles in all cases occupying compact ranges. The complex $[Fe\{(pz)_3CH\}_2][NO_3]_2$ has been defined in two independent phases, both with the above characteristics, but with the relative magnitudes of their a and b axes interchanged in the cell. One phase, denoted α, is isomorphous with its previously studied counterparts of Co, Ni, Cu and Zn; the M–N distance for iron(II) in this array (Table 3) is by far the shortest (Fig. 3) and as such may be at an extreme of sustainable lattice energy for this phase *vis-à-vis* the alternative 'β' form, the latter perhaps more stable for smaller metal ions, particularly if encouraged by some suitable crystallisation solvent. It is noteworthy, in this context, that the density of the β form is considerably greater than that of the α. It is of further interest that the already extensively defined $P2_1/n$, $Z = 2$ format carries over even further into the previously described $[M\{(py)_3N\}_2][ClO_4]_2$ array, M = Fe [17] or Co,[18b] the latter pair being isomorphous despite large differences in ⟨M–N⟩, tabulated comparatively with the present $[Fe\{(py)_3CH\}_2]^{2+}$ data in Table 4.

Small, statistically significant differences are observed in the FeN_6 geometries of the present arrays (Table 2), presumably compounded of effects due to differing constraints imposed by the ligand geometries, together with associated crystal field effects, the latter being from strong-field d^6. More considerable are changes in the angular parameters about the bridgehead, and associated variations in the angles exocyclic to the various five- and six-membered rings. Nitrate and solvent geometries are unexceptional and there are no unusual/remarkable interspecies contacts.

Electronic spectra

Solution and KBr mull spectra were measured for $[Fe\{(pz)_3CH\}_2][NO_3]_2$, $[Fe\{(py)_3CH\}_2][NO_3]_2$ and $[Fe\{(py)_3P{=}O\}_2][NO_3]_2$ (Figs. 4 and 5) and the results are summarised and compared with previously reported results for $[Fe\{(pz)_2(py)CH\}_2][NO_3]_2$ in Table 5.

The solution spectra allowed accurate measurement of absorption coefficients, but for comparing 'd–d' with charge-

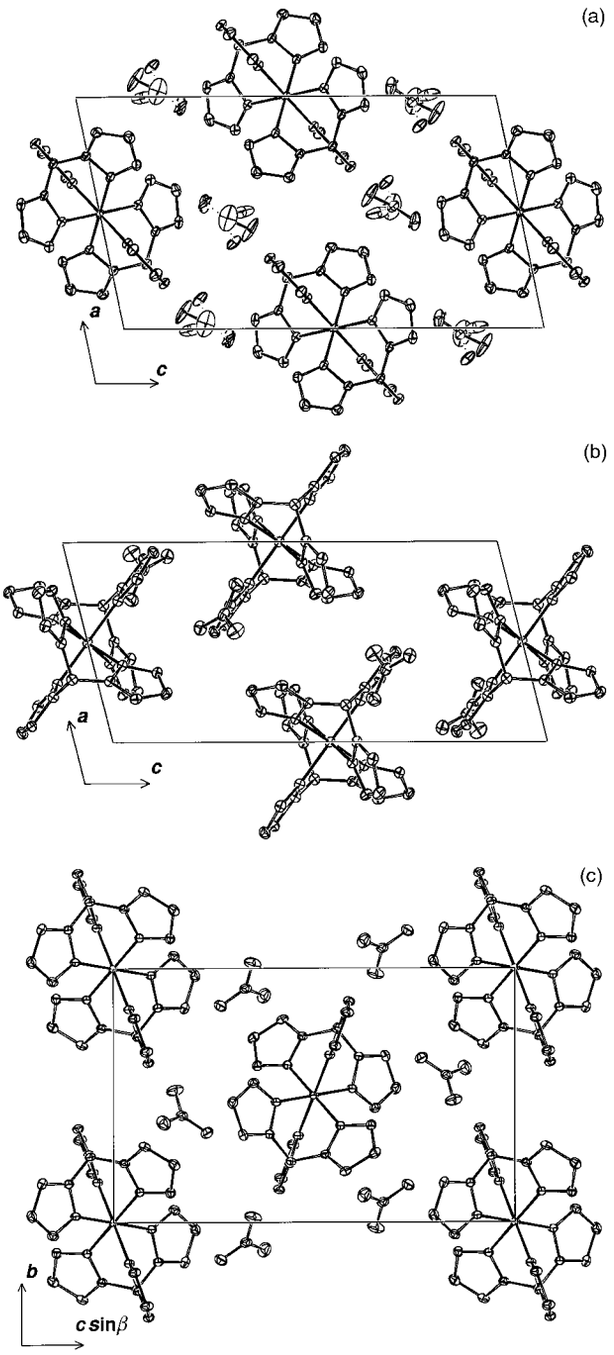

Fig. 1 (a) Unit cell contents of α-$[Fe\{(pz)_3CH\}_2][NO_3]_2$ projected down *b*; 20% thermal ellipsoids are shown here and in subsequent figures for the non-hydrogen atoms, hydrogen atoms having arbitrary radii of 0.1 Å. The unit cell contents of the β form, are projected down *b* (*b*) and *c* (*c*).

transfer (CT) transitions whose intensities were very high the KBr mull spectra provided more useful information. For $[Fe\{(pz)_3CH\}_2][ClO_4]_2$ the two lowest energy transitions which had $\varepsilon \approx 50$ dm^3 mol^{-1} cm^{-1} can be assigned to the 'd–d' transitions $^1A_{1g} \longrightarrow {}^1T_{1g}$ and $^1A_{1g} \longrightarrow {}^1T_{2g}$ respectively. The higher energy, more intense transitions are assigned as CT to the pyrazole. Small solvent shifts were noted for different salts. The $^1A_{1g} \longrightarrow {}^1T_{1g}$ transition energy is slightly higher than those noted for $[Fe\{(pz)_3BH\}_2]$[1] and $[Fe([9]aneN_3)_2]^{2+}$, a detailed analysis having recently been given for the [9]aneN$_3$ and [9]aneN$_x$S$_{3-x}$ series.[6] The CT bands for $[Fe\{(pz)_3CH\}_2]^{2+}$ are similar to those observed above 30 000 cm^{-1} for $[Fe\{(pz)_3BH\}_2]$, indicating that neither the nature of the bridgehead nor the charge on the ligand has a significant effect on the M→pyrazole transition energy.

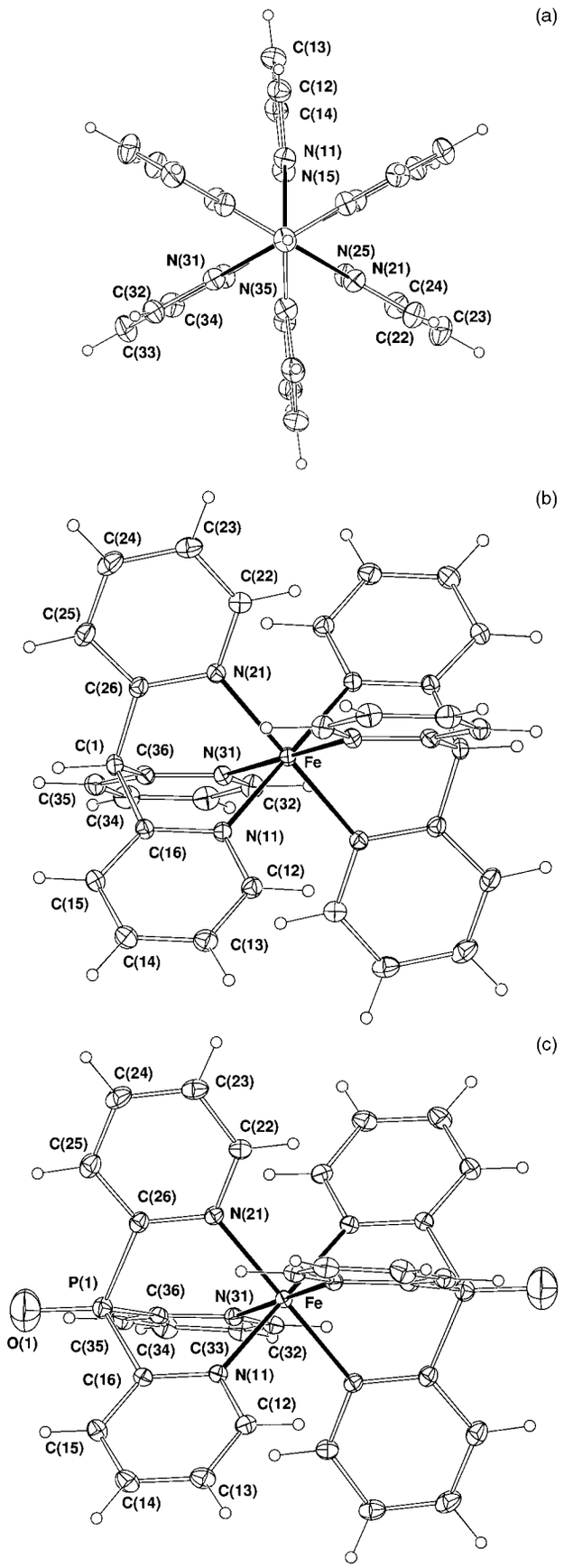

Fig. 2 Individual cations: (a) α-$[Fe\{(pz)_3CH\}_2]^{2+}$ viewed down the HC···Fe···CH axis (the β form is similar), (b) $[Fe\{(py)_3CH\}_2]^{2+}$ and (c) $[Fe\{(py)_3PO\}_2]^{2+}$.

The spectrum of $[Fe\{(py)_3CH\}_2][NO_3]_2$ shows no low intensity transitions, with all peaks having $\varepsilon > 10\,000$ dm^3 mol^{-1} cm^{-1}. Thus all transitions are assigned as CT; this is in agree-

Table 1 Crystal/refinement details for $[FeL_2][NO_3]_2$ **1**–**4**. All compounds are monoclinic, space group $P2_1/n$ (C_{2h}^5, no. 14, variant), $Z = 2$

	1 [a]	**2** [b]	**3**	**4** [c]
Formula	$[Fe\{(pz)_3CH\}_2]^{2+}$ (α) α-$C_{20}H_{20}FeN_{14}O_6$	$[Fe\{(pz)_3CH\}_2]^{2+}$ (β) β-$C_{20}H_{20}FeN_{14}O_6$	$[Fe\{(py)_3CH\}_2]^{2+}$ $C_{32}H_{26}FeN_8O_6$	$[Fe\{(py)_3PO\}_2]^{2+}$ $C_{30}H_{30}FeN_{10}O_8P_2$
M	608.3	608.3	674.5	824.5
a/Å	9.716(3)	7.739(4)	8.539(4)	11.129(3)
b/Å	7.740(2)	9.969(1)	10.405(4)	13.699(3)
c/Å	17.280(6)	16.321(2)	16.500(10)	11.239(3)
β/°	101.67(3)	104.21(3)	102.99(4)	92.04(2)
U/Å^3	1272.6(7)	1220.6(7)	1428(1)	1712.4(7)
D_c/g cm^{-3}	1.58_7	1.64_9	1.56_8	1.59_9
μ_{Mo}/cm^{-1}	6.8	7.1	5.9	6.0
Specimen/mm	0.25 × 0.22 × 0.16	0.53 × 0.29 × 0.20	0.15 × 0.18 × 0.44	Multifaceted, 0.23 mm
'T' [d] $_{min,max}$	0.87, 0.90	0.81, 0.87	0.71, 1.00	0.84, 1.00
$2\theta_{max}$/°	50	60	55	55
N	2240	3536	3606	4264
N_o	1786	2354	2592	2496
R	0.047	0.044	0.037	0.048
R_w	0.056	0.045	0.044	0.054
$\|\Delta\rho_{max}\|$/e Å^{-3}	0.5	0.5	0.4	0.5

[a] This form is presented in the same cell and coordinate setting as for the previously described cobalt, nickel, copper and zinc analogues (ref. 17). The nitrate was modelled with the oxygen atoms disordered over two sets of sites about the nitrogen, occupancies set at 0.5 after trial refinement. [b] The cell of the $P2_1/c$ setting of the β polymorph has very similar dimensions to that of the $P2_1/n$ setting. [c] This compound is an acetonitrile disolvate. [d] **1**, **2**, Gaussian correction; **3**, **4**, 'empirical' correction.[18a]

Table 2 Selected cation geometries (X = capping atom) (independent values), distances in Å, angles in °. All iron atoms are located on crystallographic inversion centres

Cation	**1** (α-)$[Fe\{(pz)_3CH\}_2]^{2+}$	**2** (β-)$[Fe\{(pz)_3CH\}_2]^{2+}$	**3** $[Fe\{(py)_3CH\}_2]^{2+}$	**4** [a] $[Fe\{(py)_3PO\}_2]^{2+}$
Fe–N(11)	1.975(3)	1.963(2)	1.954(2)	1.980(4)
Fe–N(21)	1.966(3)	1.957(3)	1.947(2)	1.982(3)
Fe–N(31)	1.963(3)	1.957(2)	1.947(2)	1.984(3)
⟨Fe–N⟩	1.968(5)	1.959(3)	1.949(3)	1.982(2)
N(11)–Fe–N(21)	87.7(1)	87.1(1)	89.07(7)	91.7(1)
N(11)–Fe–N(31)	87.1(1)	87.96(9)	88.99(7)	92.0(1)
N(21)–Fe–N(31)	88.0(1)	87.7(1)	89.20(8)	91.9(1)
Fe–N(11)–N(15),C(16)	117.0(2)	118.1(2)	118.9(1)	122.4(3)
Fe–N(21)–N(25),C(26)	118.2(2)	118.1(2)	118.8(1)	122.3(3)
Fe–N(31)–N(35),C(36)	118.4(2)	118.2(2)	118.8(2)	121.9(3)
Fe–N(11)–C(12)	137.0(3)	136.6(2)	123.5(1)	121.6(3)
Fe–N(21)–C(22)	136.8(3)	137.4(2)	123.6(2)	120.8(3)
Fe–N(31)–C(32)	137.5(3)	137.0(2)	123.7(2)	121.8(3)
N(15)/C(16)–X–N(25)/C(26)	110.8(3)	108.8(2)	109.3(2)	101.2(2)
N(25)/C(26)–X–N(35)/C(36)	108.9(3)	110.0(2)	110.8(2)	103.2(2)
N(35)/C(36)–X–N(15)/C(36)	109.7(3)	109.7(2)	111.1(2)	101.2(2)

[a] O–P–C(16,26,36) are 118.1(3), 116.0(3), 114.8(3)°.

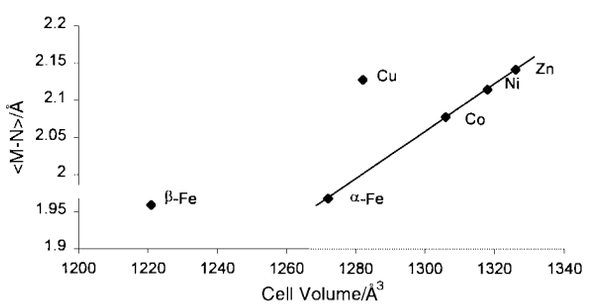

Fig. 3 Comparison of unit cell volumes (Å^3) and average metal to ligand bond lengths (Å).

ment with Angular Overlap Model calculations which indicate that the 'd–d' transitions should be expected at ≈20 000 cm^{-1} and thus would be masked by the intense CT band. Unidentate iron(II) pyridine complexes show CT transitions between 24 000 and 26 000 cm^{-1},[21] whereas pyrazole containing ligands have CT transitions at much higher energy (>29 000 cm^{-1}).[22] The CT transition of $[Fe(bipy)_3]^{2+}$ is at slightly lower energy (19 160 cm^{-1}).[23]

The spectra of $[Fe\{(py)_3P{=}O\}_2][NO_3]_2$ are similar to those of $[Fe\{(py)_3CH\}_2][NO_3]_2$, with slight shifts to lower energy (22 800 to 21 500 and 27 000 to 26 000 cm^{-1}) presumably resulting from the replacement of the carbon bridgehead by phosphine oxide.

The previously reported spectra[4] of $[Fe\{(pz)_2(py)CH\}_2][NO_3]_2$ showed intense peaks ($\varepsilon \approx 2000$ dm^3 mol^{-1} cm^{-1}) at 23 400 and 31 000 cm^{-1} which were tentatively assigned to M→L CT transitions. The spectra of the $(py)_3CH$ and $(pz)_3CH$ complexes confirm these assignments as CT transitions to the pyridine and pyrazole ring moieties respectively. A low temperature crystal spectrum indicated shoulders at ≈24 400 and 26 200 cm^{-1} which were tentatively assigned as 'd–d' transitions. The spectrum of the $(pz)_2(py)CH$ complex is essentially a superposition of the $(pz)_3CH$ and $(py)_3CH$ spectra, confirming that there is no conjugation between the rings in such tripod ligands. When conjugation is possible, as for the $(py)_3P{=}O$ complex, the CT band shifts slightly to lower energy. All spectra are consistent with the iron(II) complexes being low spin, with angular overlap calculations[4] suggesting a Δ splitting for the $(pz)_3CH$ complex of ≈23 000 cm^{-1}. This is almost twice that reported for the analogous nickel complex (11 840 cm^{-1}) in keeping with the shorter Fe–N bonds. The very small fraction

Table 3 Isomorphous $[M\{(pz)_3CH\}_2][NO_3]_2$ (α phase) comparative geometries (distances in Å, angles in °)

	Fe	Co[a]	Ni[a]	Cu[a]	Zn[a,b]
M–N(11)	1.975(3)	2.114(3)	2.077(2)	2.028(2)	2.145(3)
M–N(21)	1.966(3)	2.108(3)	2.072(2)	2.001(2)	2.130(2)
M–N(31)	1.963(3)	2.122(2)	2.084(2)	2.355(2)	2.150(2)
⟨M–N⟩	1.968(5)	2.115(6)	2.078(5)	2.13(16)	2.142(8)
N(11)–M–N(21)	87.7(1)	84.6(1)	85.5(1)	86.8(1)	84.3(1)
N(11)–M–N(31)	87.1(1)	83.7(1)	84.6(1)	81.5(1)	83.3(1)
N(21)–M–N(31)	88.0(1)	85.3(1)	86.2(1)	86.1(1)	85.2(1)

[a] Ref. 17. [b] Ref. 19.

Table 4 $[M\{(py)_3X\}_2]^{2+}$ (X = CH or N) comparative geometries (distances in Å, angles in °)

X/anion	CH/NO_3^-	N/ClO_4^-	
M	Fe	Fe[a]	Co[b]
M–N(11)	1.954(2)	1.981(4)	2.111(2)
M–N(21)	1.947(2)	1.970(5)	2.100(2)
M–N(31)	1.947(2)	1.995(5)	2.152(2)
⟨M–N⟩	1.949(3)	1.98(1)	2.12(2)
N(11)–M–N(21)	89.07(7)	88.5(2)	86.09(8)
N(11)–M–N(31)	88.99(7)	88.1(2)	85.74(8)
N(21)–M–N(31)	89.20(8)	87.8(2)	84.86(7)
C(16)–X–C(26)	109.3(2)	111.7(5)	113.7(2)
C(16)–X–C(36)	110.8(2)	111.7(5)	112.9(2)
C(26)–X–C(36)	111.1(2)	111.0(4)	112.7(2)

[a] Ref. 20(*a*). [b] Ref. 20(*b*).

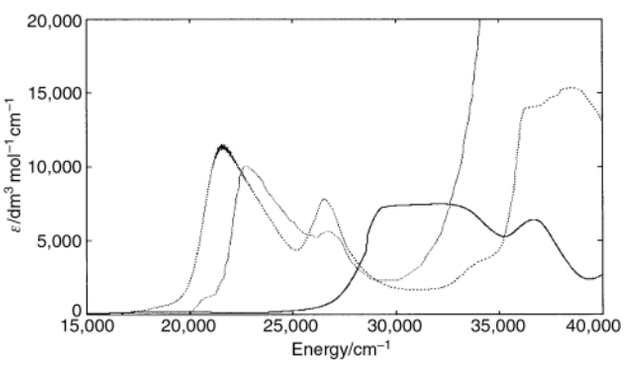

Fig. 4 Solution spectra in acetonitrile for $[Fe\{(pz)_3CH\}_2][ClO_4]_2$ (solid), $[Fe\{(py)_3CH\}_2][NO_3]_2$ (light) and $[Fe\{(py)_3PO\}_2][NO_3]_2$ (dashed).

of $[Fe\{(pz)_3CH\}_2]^{2+}$ present in the high-spin state at 295 K (see following section) was not detected in the optical spectrum.

Magnetic susceptibilities and Mössbauer effect

The spin states of $[Fe^{III}\{(pz)_3CH\}_2][ClO_4]_3$ at 295 K and $[Fe^{II}\{(pz)_3CH\}_2][ClO_4]_2$ at 4.2 K were confirmed as low-spin d^5 and d^6, respectively, by the use of Mössbauer spectroscopy. Isomer shift (δ) and quadrupole splitting (ΔE_Q) values for the well resolved quadruple doublets were 0.052, $\Delta E_Q = 0.820$ (Fe^{III}) and 0.488, $\Delta E_Q = 0.248$ mm s^{-1} (Fe^{II}). Winkler *et al.* obtained similar values for $[Fe^{II}\{(pz)_3CH\}_2][PF_6]_2$ in a study of the rapid spin state interconversion rate which occurred above 300 K.[3] For comparison, $[Fe^{II}\{(pz)_3BH\}_2]$ showed $\delta = 0.48$, $\Delta E_Q = 0.20$ mm s^{-1}[24] while $[Fe^{II}([9]aneNS_2)_2][ClO_4]_2$ showed $\delta = 0.43$, $\Delta E_Q = 0.28$ mm s^{-1}, both at 4.2 K.[6] Above 295 K, $[Fe\{(pz)_3BH\}_2]$ showed increased population of the high-spin state and effective relaxation rates for spin state interconversion were very similar to those for $[Fe\{(pz)_3CH\}_2][PF_6]_2$.[3,24]

The magnetic moment for $[Fe^{III}\{(pz)_3CH\}_2][ClO_4]_3$ decreases gradually from 2.9 μ_B at 300 K to 2.0 μ_B at 4.2 K in a manner

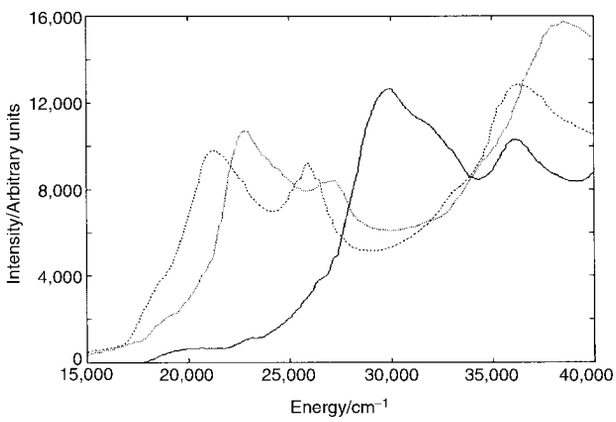

Fig. 5 Electronic spectra of KBr mulls measured at 15 K for $[Fe\{(pz)_3CH\}_2][NO_3]_2$ (solid), $[Fe\{(py)_3CH\}_2][NO_3]_2$ (light) and $[Fe\{(py)_3PO\}_2][NO_3]_2$ (dashed).

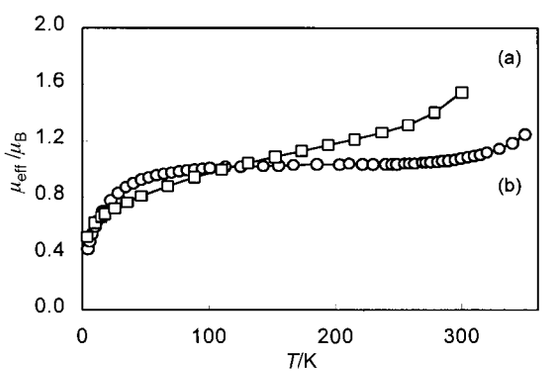

Fig. 6 Plots of μ_{Fe} *versus* temperature, in a field of 1 T, for (a) $[Fe\{(pz)_3CH\}_2][ClO_4]_2$ and (b) β-$[Fe\{(pz)_3CH\}_2][NO_3]_2$.

anticipated for a trigonally distorted $^2T_{2g}$ state with a negative spin–orbit coupling constant.[25] There is no hint of any spin change to high spin ($^6A_{1g}$) occurring below 300 K. The behaviour is similar to that of a 1-thia-4,7-diazacyclononane complex $[Fe^{III}([9]aneN_2S)_2][ClO_4]_3$.[6]

The iron(II) complex $[Fe\{(pz)_3CH\}_2][ClO_4]_2$ showed evidence of a gradual spin change from low to high spin beginning above ≈270 K (Fig. 6). The μ_{Fe} value of 1.51 μ_B at 300 K is indicative of a high-spin population of about 7%.[2] Below 270 K the μ_{Fe} values decreased slowly towards 0.8 μ_B at 50 K and 0.5 μ_B at 4.2 K. These low values of μ_{Fe} originate mainly from the $^1A_{1g}$ (diamagnetic) state plus a second-order Zeeman derived temperature independent susceptibility (TIP) and not from any residual iron(III) species, the latter being absent in the Mössbauer spectrum. The β polymorph of $[Fe\{(pz)_3CH\}_2][NO_3]_2$ showed a slightly different temperature dependence of μ_{Fe} over the range 4–350 K with μ_{Fe} being essentially constant at 1.05 μ_B between 50 and 270 K and then increasing a little, gradually, to 1.26 μ_B at 350 K (Fig. 6). Physical effects such as crystallite size and sample grinding might affect such data. It is likely, however, that variation in the anion plays a part in these

Table 5 Spectroscopic results for the $[Fe^{II}(ligand)_2]^{2+}$ complexes studied. Transition energies (cm^{-1}) and absorption coefficients ($dm^3\ mol^{-1}\ cm^{-1}$) in brackets where known

	Ligand			
Assignment	$(pz)_3CH$ (α form)	$(py)_3CH$	$(py)_3P{=}O$	$(pz)_2(py)CH$ [a]
d–d	19 200 (56) [b]	—	—	—
	23 250 [c]			
Unknown				24 400
				26 200
CT to py	—	22 800 (10 700)	21 500 (12 000)	23 400 (2000)
CT to pz	30 000	—	—	31 000 (2000)
Other CT	36 350	27 000	26 000 (8000)	38 000
		37 500	36 000 (15 000)	

[a] Ref. 4. [b] Measured as the ClO_4^- salt. The NO_3^- salt dissolved in DMF gave a transition at 19 760 cm^{-1}. [c] Measured from an arbitrary face of a single crystal using polarised light at 15 K.

solid state data, as found in other crossover systems, particularly those involving chelates of iron(III).[24] Unfortunately we have not been able to obtain enough of the α isomer to measure its magnetic properties for comparison. As indicated in the Experimental section, repeat preparations of it led to the β form being produced. We do not have variable temperature data on solid samples of the pyridyl complexes **3** and **4**, but visible spectra and magnetic moments on these and on $[Fe\{(pz)_2(py)CH\}_2][NO_3]_2$ show that they are fully low spin at room temperature.[4] The small differences noted in the Fe–N distances (Table 4) can not be correlated with any differences in magnetic properties.

The analogous complex $[Fe\{(pz)_3BH\}_2]$ also showed low-spin behaviour in the solid state up to 280 K and then a gradual change to 4.91 μ_B at 461 K, typical of the high-spin state. A crystallographic phase transition accompanying the spin crossover occurs upon heating, at 400 K.[24] The spin state in the hydrotris(pyrazol-1-yl)borate series is sensitive to substitution on the pyrazole rings, the 3,5-dimethyl derivatives being high spin at all temperatures.[1] Other iron(II) bis- and tris-pyrazolylmethane complexes are known to display different spin states depending on Fe to ligand stoichiometry and the presence of other co-ordinated ligands such as NCS^-.[22]

Conclusion

The electronic spectra of the tripodal ligand series $[Fe^{II}L_2]^{2+}$, where L = $(pz)_3CH$, $(pz)_2(py)CH$, $(py)_3CH$ or $(py)_3P{=}O$, are dominated by metal→ligand charge transfer transitions, with the complexes formed by the ligands containing pyridine being at significantly lower energy. The spectrum of the complex formed by the $(pz)_2(py)CH$ ligand was essentially a superposition of the spectra of complexes of the ligands involving just one type of amine. While one of the two crystal modifications of $[Fe\{(pz)_3CH\}_2]^{2+}$ is similar to that adopted by other divalent transition ions, a second, dominant β modification is also observed for this metal ion. This is denser than the α form, and the fact that it is adopted by Fe^{2+} may be related to the small ionic radius of this metal ion in the low-spin state. Magnetic and Mössbauer studies on the solid $[Fe\{(pz)_3CH\}_2]^{2+}$ samples show that spin crossover occurred, in a gradual fashion, above *ca.* 270 K. In order to access both spin states, it will be necessary finely to tune substituent groupings on the pyrazole rings. Indeed, we have just learned that Reger *et al.*[25] have observed unusual spin-crossover behaviour in $[Fe\{(3,5\text{-}Me_2pz)_3CH\}_2][BF_4]_2$. The dynamics of spin crossover for $[Fe\{(pz)_3CH\}_2][PF_6]_2$, above 300 K, is very similar to that for $[Fe\{(pz)_3BH\}_2]$.[2,24] Thus changing CH for BH, and the charge, in these pyrazolyl-based ligands has little effect.

Acknowledgements

We thank the Australian Research Council for support of the crystallographic facilities at the University of Adelaide and Western Australia. ARC Large grants supported the magnetochemistry work at Monash University, the synthetic and electrochemical studies at James Cook University, and the spectroscopic work at the University of Tasmania. Associate Professor J. D. Cashion and Mr R. Mackie (Monash University) and Dr S. Nakashima (Hiroshima University) are thanked for their contribution to the work.

References

1 J. P. Jesson, S. Trofimenko and D. R. Eaton, *J. Am. Chem. Soc.*, 1967, **89**, 3158.
2 J. J. McGarvey, H. Toftlund, A. H. R. Al-Obaidi, K. P. Taylor and S. E. J. Bell, *Inorg. Chem.*, 1993, **32**, 2469.
3 H. Winkler, A. X. Trautwein and H. Toftlund, *Hyperfine Interact.*, 1992, **70**, 1083.
4 T. Astley, A. J. Canty, M. A. Hitchman, G. L. Rowbottom, B. W. Skelton and A. H. White, *J. Chem. Soc.*, *Dalton Trans.*, 1991, 1981.
5 F. R. Keene, M. R. Snow, P. J. Stephenson and E. R. T. Tiekink, *Inorg. Chem.*, 1988, **27**, 2040; T. A. Hafeli and F. R. Keene, *Aust. J. Chem.*, 1988, **41**, 1379.
6 V. A. Grillo, L. R. Gahan, G. R. Hanson, R. Stranger, T. W. Hambley, K. S. Murray, B. Moubaraki and J. D. Cashion, *J. Chem. Soc.*, *Dalton Trans.*, 1999, 2341.
7 G. D. Fallon, S. Knight, B. Moubaraki, K. S. Murray, B. W. Skelton and A. H. White, *J. Inorg. Biochem.*, 1993, **51**, 504.
8 S. Trofimenko, *J. Am. Chem. Soc.*, 1970, **92**, 5118.
9 P. K. Byers, A. J. Canty and R. T. Honeyman, *J. Organomet. Chem.*, 1990, **385**, 417.
10 B. Moubaraki, K. S. Murray, E. R. T. Tiekink and K. Van Langenberg, unpublished data.
11 M. A. Hitchman, *Transition Met. Chem.* (*New York*), 1985, **9**, 1.
12 S. R. Hall and J. M. Stewart (Editors), *The Xtal 3.0 Reference Manual*, University of Western Australia, 1990.
13 TEXSAN, Structure Analysis Package, Molecular Structure Corporation, Houston, TX, 1992.
14 B. F. Abrahams, K. D. Lu, B. Moubaraki, K. S. Murray and R. Robson, *J. Chem. Soc.*, *Dalton Trans.*, 2000, 1793.
15 S. Decurtins, A. W. Schmalle, P. Schneuwly and H. R. Oswald, *Inorg. Chem.*, 1993, **32**, 1888.
16 C.-T. Lin, W. Böttcher, M. Chou, C. Creutz and N. Sutin, *J. Am. Chem. Soc.*, 1976, **98**, 6536.
17 T. Astley, J. M. Gulbis, M. A. Hitchman and E. R. T. Tiekink, *J. Chem. Soc.*, *Dalton Trans.*, 1993, 509.
18 (*a*) N. Walker and D. Stuart, *Acta Crystallogr.*, *Sect. A*, 1983, **39**, 158; (*b*) T. Astley, P. J. Ellis, H. C. Freeman, M. A. Hitchman, F. R. Keene and E. R. T. Tiekink, *J. Chem. Soc.*, *Dalton Trans.*, 1995, 595; T. Astley, H. Headlam, M. A. Hitchman, F. R. Keene, J. Pilbrow, H. Stratemeier, E. R. T. Tiekink and Y. Zhong, *J. Chem. Soc.*, *Dalton Trans.*, 1995, 3809.
19 E. S. Zvargulis, I. E. Biys and T. W. Hambley, *Polyhedron*, 1995, **14**, 2267.
20 (*a*) E. S. Kuchorski, W. R. McWhinnie and A. H. White, *Aust. J. Chem.*, 1978, **31**, 53; (*b*) E. S. Kuchorski, W. R. McWhinnie and A. H. White, *Aust. J. Chem.*, 1978, **31**, 2647.
21 N. Sanders and P. Day, *J. Chem. Soc. A*, 1969, 2303.
22 F. Mani, *Inorg. Nucl. Chem. Lett.*, 1979, **15**, 297.

23 F. Felix, J. Ferguson, H. U. Güdel and A. Ludi, *Chem. Phys. Lett.*, 1979, **62**, 153.
24 F. Grandjean, G. J. Long, B. B. Hutchinson, L. Ohlhausen, P. Neill and J. D. Holcomb, *Inorg. Chem.*, 1989, **28**, 4406.
25 F. E. Mabbs and D. J. Machin, *Magnetism and Transition Metal Complexes*, Chapman and Hall, London, 1973, ch. 5.
26 B. J. Kennedy, A. C. McGrath, K. S. Murray, B. W. Skelton and A. H. White, *Inorg. Chem.*, 1987, **26**, 483; M. D. Timken, A. M. Abdel-Mawgoud and D. N. Hendrickson, *Inorg. Chem.*, 1986, **25**, 160; E. V. Dose, K. M. M. Murphy and L. J. Wilson, *Inorg. Chem.*, 1976, **15**, 2622.
27 D. L. Reger, C. A. Little, A. L. Rheingold, M. Lam, T. Concolino, A. Mohan and G. J. Long, *Inorg. Chem.*, in press; D. L. Reger, personal communication, February 2000.